

doi: 10.13241/j.cnki.pmb.2017.25.041

弹性成像技术在子宫肌瘤射频治疗中的应用价值 *

段景域 董晓秋[△] 张立维 孔德娇 邵小慧

(哈尔滨医科大学附属第四医院超声科 黑龙江哈尔滨 150001)

摘要 目的:探讨实时超声弹性成像(Real-time ultrasound elastography, RTE)在子宫肌瘤射频消融治疗(radiofrequency ablation, RFA)中的应用价值。**方法:**对34例行RFA治疗的子宫肌瘤患者(共38个病灶)于术前、术后1小时、术后3个月进行阴式超声、RTE及超声造影(contrast-enhanced ultrasonography, CEUS)检查。在2D、RTE、CEUS三种条件下分别测量病灶的直径。分析术前弹性图特征并分组,测量病灶弹性应变比率(E/E_0),对比分析组间、组内的 E/E_0 。比较2D、RTE、CEUS条件下病灶直径之间的差异。术后以弹性图像上病灶显示蓝绿相间为判定消融不全的标准,与CEUS对比,分析RTE与CEUS对消融程度评估的一致性。**结果:**根据术前肌瘤弹性图像将病灶分为蓝色组8个(21.1%),蓝色为主组20个(52.6%),绿色为主组10个(26.3%),术前3组病灶之间 E/E_0 差异明显,术后1小时、术后3个月 E/E_0 差异无统计学意义($P>0.05$),组内RFA术后1小时、3个月病灶 E/E_0 较术前明显增大,术后3个月 E/E_0 大于术后1小时($P<0.05$);术前RTE检测病灶直径大于2D及CEUS($P<0.05$),术后1小时2D测量直径大于RTE及CEUS($P<0.05$),三种成像技术在术后3个月测量病灶直径差异无统计学意义($P>0.05$);RFA术后1小时及术后3个月RTE对病灶消融程度评估结果与CEUS基本一致,Kappa值分别为0.46、0.54。**结论:**RFA术后肌瘤逐步变硬,RTE检查能够反映这种硬度变化,并且能够评估消融病灶的范围并预估消融程度,因此RTE在子宫肌瘤RFA治疗中有一定的应用价值。

关键词:子宫肌瘤;射频治疗;弹性成像

中图分类号:R445.1;R711.74 文献标识码:A 文章编号:1673-6273(2017)25-4967-04

Application Value of Ultrasound Elastography Techniques in the Treatment of Uterine Fibroids Radiofrequency Ablation*

DUAN Jing-yu, DONG Xiao-qiu[△], ZHANG Li-wei, KONG De-jiao, SHAO Xiao-hui

(Department of Ultrasonography, the fourth Affiliated Hospital of Harbin Medica University, Harbin, Heilongjiang, 150001, China)

ABSTRACT Objective: To investigate the application value of real-time ultrasound elastography in the treatment of fibroids radiofrequency ablation (RFA). **Methods:** Transvaginal ultrasonography, Real-time ultrasound elastography (RTE) and contrast-enhanced ultrasonography (CEUS) were performed on 34 patients with a total of 38 uterine fibroids who had the treatment of RFA before, 1 hour and 3 months after the treatment of RFA. Detected the diameters of the lesions with the three methods of CEUS, RTE and 2D. Analysed the elastic image features and divided into groups, Measured the elastic strain ratio and compared the E/E_0 in and between the group. The difference of lesion diameter between 2D, RTE and CEUS was compared. When the image of lesions showed blue and green was taken as the criterion of incomplete ablation after RFA, compared with CEUS, analysed the consistency of RTE and CEUS in evaluating the degree of ablation. **Results:** The lesions were divided into 3 groups according to the preoperative elastic image, with 8 (21.1%) in the blue group, 20 (52.6%) in blue-based and 10 (26.3%) in green-based group. The difference was obvious in E/E_0 between the 3 groups before RFA. There was no significant difference in E/E_0 between 1 hour and 3 months after RFA ($P>0.05$). In each group the E/E_0 of lesions were significantly increased at 1 hour and 3 months after the treatment of RFA, and the hardness of 3 months after RFA was harder than that of 1 hour after RFA($P<0.05$). The diameter measured by RTE was larger than that by 2D and CEUS before RFA($P>0.05$). The diameter measured by 2D was larger than that by RTE and CEUS at 1 hour after RFA ($P<0.05$). No statistically significant difference was found in the lesion diameters among the three methods of 2D, RTE and CEUS at 3 months after the treatment of RFA ($P>0.05$). CEUS and RTE had the basic consistent in the evaluation of lesions ablation degree at 1 hour ($\kappa=0.46$) and 3 months ($\kappa=0.54$) after the treatment of RFA. **Conclusions:** After RFA, the myoma gradually hardens, and RTE can reflect the change of the hardness, RTE can clearly show the boundary of uterine fibroids especially after the treatment of RFA, can be used in the prediction of lesions ablation degree, so there was a certain application value of RTE used in RFA.

Key words: Uterine fibroids; Radiofrequency ablation; Real-time ultrasound elastography

Chinese Library Classification(CLC): R445.1; R711.74 **Document code:** A

Article ID: 1673-6273(2017)25-4967-04

* 基金项目:国家自然科学基金项目(81271646)

作者简介:段景域(1990-),硕士研究生,电话:13845166343,E-mail:1135762679@qq.com

△ 通讯作者:董晓秋,博士,硕士生导师,主任医师,主要研究方向:腹部、妇产科及小器官的超声诊断与介入治疗,

电话:(0451)82576705,E-mail:dongxq0451@163.com

(收稿日期:2017-03-11 接受日期:2017-04-08)

前言

子宫肌瘤是女性生殖系统最常见的良性肿瘤,30-50岁的女性发病率约为20%^[1]。RFA是在超声的引导及监视下将自凝刀置于病灶内部,致病灶局部产生生物高热效应,使病灶发生凝固性坏死,以改善患者临床症状,提高患者生活质量的微创治疗方法。该方法用于子宫肌瘤的治疗较传统外科手术而言具有创伤小,安全性高,治疗费用低,临床效果确切等优点^[2]。目前临幊上对于热消融病灶的评估常以增强CT、MRI作为影像学评估的金标准,而近年来CEUS用于消融病灶评估方面的价值也得到了广大学者的认可并在临幊广泛应用^[3-5]。但以上方法存在价格昂贵、有创、操作复杂等不足。本研究旨在探讨RTE在子宫肌瘤RFA中的应用价值。

1 资料与方法

1.1 临床资料

收集2014年9月至2016年4月在我院自愿接受RFA治疗的肌壁间肌瘤患者34例,共38个病灶,年龄31-52岁,平均(42.2±4.7)岁,肌瘤直径≤5cm,平均(3.4±0.9)cm,且肌瘤中心点距阴式探头距离≤3cm。所有患者均已婚且无再生育要求,无其他妇科疾病,无凝血功能障碍和心脏病等手术禁忌症。术前向患者及家属详细交待手术过程及术中可能出现的风险、术后并发症等,签署知情同意书。

1.2 仪器与方法

1.2.1 仪器与药品 应用配备有RTE软件的Logiq E9彩色多普勒超声诊断仪,具有低机械指数实时谐波超声造影功能。腹部探头频率1.0-5.0MHz,阴式探头频率5.0-9.0MHz。RFA治疗采用BBT-RF-E妇科多功能射频治疗仪,工作频率(550±40)kHz,最大输出功率为50W。造影剂为声诺维(SonoVue),使用时加入5mL注射用生理盐水,用力振摇混匀后,抽取2.4mL微泡混悬液以团注方式经肘前静脉快速注入,随后推注5mL生理盐水冲注。

1.2.2 方法 全部病例在RFA治疗前、术后1小时及术后3

个月行阴道二维超声检查。观察肌瘤位置、数量、回声水平、血流情况并测量其最大直径。在阴式超声检查基础上加用RTE技术。取样框范围尽可能包括全部病灶及部分周边正常组织。手持探头在病灶部位做微小振动,位置高的肌瘤配合腹部加压,待压力质量指示标尺变为绿色,压力曲线频率及幅度均匀,弹性图像稳定时冻结图像,弹性图像上由红到蓝代表组织由软到硬,观察病灶弹性图特征并分组,利用机身自带的弹性测量方法选取病灶区域(E)和相邻正常肌组织区域(E₀),感兴趣区要尽量等大且保持在同一深度,计算E/E₀,并且测量弹性图上肌瘤最大直径。RFA治疗前、术后1小时及术后3个月行CEUS。观察病灶造影剂灌注情况,于平衡期时测量病灶最大直径。消融程度判定标准是肌瘤内部无造影剂灌注为完全消融,反之,为消融不全^[6],对于术后1小时消融不全者,再次补针消融。术后1小时E/E₀结果以补充消融后为准。所有测值均测量三次取平均值。

1.2.3 RFA治疗 患者取截石位,将电极板置于腰骶部,射频治疗仪功率设置为20-40W,根据肌瘤大小、位置、肌瘤血供情况制定个性化消融方案,在经腹超声引导下经阴道进入自凝刀进行RFA治疗。

1.3 统计方法

用SPSS 23.0统计软件包对数据进行处理。计量资料以均数±标准差(±s)表示,以P<0.05为差异有统计学意义。多组间数据采用方差分析。以Kappa值评价RTE与CEUS评估病灶消融程度的一致性,Kappa>0.75为高度一致,0.75≥Kappa≥0.4为基本一致,Kappa<0.4为一致性差。

2 结果

2.1 肌瘤病灶E/E₀的比较

根据术前弹性图特征将病灶分为3组,蓝色组8个(21.1%),蓝色为主组20个(52.6%),绿色为主组10个(26.3%),术前组间E/E₀差异明显,术后1小时及3个月差异无统计学意义(P>0.05),组内RFA术后1小时、3个月病灶E/E₀较术前明显增大,术后3个月E/E₀大于术后1小时(P<0.05),见表1。

表1 不同弹性特征病灶的E/E₀(±s)
Table 1 E/E₀ of different elastic characteristics of lesions(±s)

| Groups | Number of lesions(%) | Before RFA | 1 hour after RFA | 3 months after RFA | P |
|-------------|----------------------|------------|------------------|--------------------|-------|
| Green-based | 10(26.3) | 1.5±0.4 | 3.5±0.4 | 3.9±0.4 | <0.05 |
| Blue-based | 20(52.6) | 2.5±0.3 | 3.4±0.3 | 3.8±0.4 | <0.05 |
| Blue | 8(21.1) | 3.1±0.3 | 3.6±0.3 | 4.1±0.3 | <0.05 |
| P | | <0.05 | >0.05 | >0.05 | |

2.2 2D、RTE、CEUS三种方法测量病灶直径的比较

术前RTE测量病灶直径大于2D及CEUS(P<0.05),术后1小时2D测量直径大于RTE及CEUS(P<0.05),三种成像方法在术后3个月测量病灶直径差异无统计学意义(P>0.05),见表2、图1、图2。

2.3 术后1小时及3个月RTE与CEUS对病灶消融情况评估结果(补充消融前)的比较

RFA术后1小时及术后3个月RTE对病灶消融情况评估结果与CEUS基本一致(Kappa值分别为0.47、0.54),见表3。

3 讨论

1991年由O'phir^[7]等提出了超声弹性成像概念,它是根据不同组织的弹性系数差异进行成像的一种技术。近年来发展的RTE成像原理是将组织内部的弹性模量等力学属性的差异示以不同颜色,以直观显示不同组织的相对硬度。目前,RTE在鉴别乳腺、甲状腺等浅表器官肿瘤良、恶性中的价值已得到证实^[8-10]。子宫肌瘤是由增生的平滑肌细胞和数量不等的纤维结缔组织细胞构成,理论上其硬度较正常子宫肌层硬,国内外亦有

研究表明,典型的子宫肌瘤弹性图像表现为肌瘤内部以蓝色为主^[11,12]。RFA 治疗使肌瘤组织升温,使肌瘤细胞发生脱水、蛋白变性、凝固性坏死^[13],消融病灶硬度与周边正常组织差异增大。

理论上 RTE 能反映这种变化,并可以用来评价子宫肌瘤消融范围及消融程度。但是,RTE 用于子宫肌瘤热消融治疗前、后的研究目前尚处于离体及动物实验阶段^[14,15]。

表 2 2D、RTE、CEUS 技术显示病灶直径的比较(cm, $\bar{x} \pm s$)Table 2 Comparison of diameter by 2D, RTE and CEUS (cm, $\bar{x} \pm s$)

| Methods | Before RFA | 1 hour after RFA | 3 months after RFA |
|---------|------------------------|------------------|--------------------|
| 2D | 3.3± 0.9 ¹ | 3.7± 0.9*# | 2.0± 0.9 |
| RTE | 3.6± 0.8 ¹² | 3.6± 0.9* | 1.9± 0.9 |
| CEUS | 3.4± 0.9 ² | 3.5± 0.9* | 1.9± 0.9 |

Note: 1,2,*; #P<0.05.

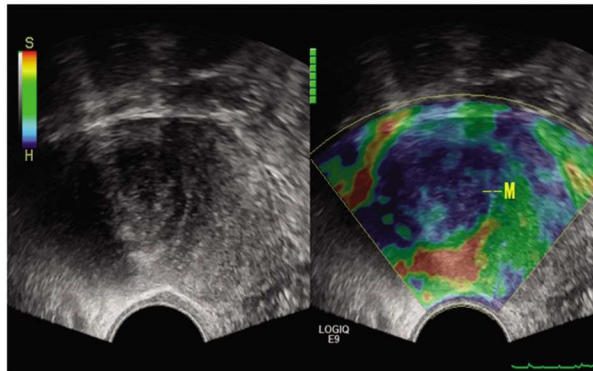


图 1 RFA 术后 1 小时 RTE

Fig.1 RTE at one hour after RFA

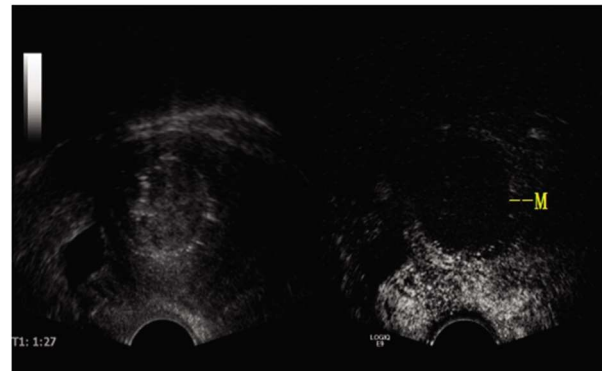


图 2 RFA 术后 1 小时 CEUS

Fig.2 CEUS at one hour after RFA

表 3 术后 1 小时及 3 个月 RTE 与 CEUS 比较(n=38)

Table 3 Comparison of RTE and CEUS at 1 hour and 3 months after RFA

| RTE | Number of lesions | CEUS of 1 hour after RFA | | Number of lesions | CEUS of 3 months after RFA | |
|-------------------|-------------------|--------------------------|----------------------|-------------------|----------------------------|----------------------|
| | | No perfusion | Uneven hypoperfusion | | No perfusion | Uneven hypoperfusion |
| Blue | 32 | 29 | 3 | 33 | 31 | 2 |
| Blue and green | 6 | 2 | 4 | 5 | 2 | 3 |
| Number of lesions | 38 | 31 | 7 | 38 | 33 | 5 |

Note: 1 hour after RFA Kappa=0.46, 3 months after RFA Kappa=0.54.

本研究中根据术前肌瘤弹性图特征将其分为三组,蓝色组占 21.1%,蓝色为主占 52.6%,绿色为主者占 26.3%,组间术前 E/E₀ 差异明显。既往研究表明^[16,17],子宫肌瘤的硬度与平滑肌细胞、结缔组织含量的多少及肌瘤细胞的排列方式关系密切。肌瘤细胞以束状排列为主,间质水肿,质地相对较软,病灶呈现以绿色为主,E/E₀ 小;肌细胞呈编织状交替排列,含纤维支架成分较多,排列规则,则质地较硬,病灶呈现以蓝色为主,E/E₀ 较大。但无论术前病灶软硬,术后 1 小时、术后 3 个月消融灶呈现完全被蓝色覆盖或以蓝色为主,E/E₀ 较术前均明显升高,且术后 3 个月 E/E₀ 较术后 1 小时升高更明显,分析原因与 RFA 治疗术后病灶的病理演变过程相关。RFA 术后,肌瘤细胞脱水、凝固性坏死,故硬度增加,随时间继续推移,坏死组织分解和液化,遗留下的组织缺损区由肉芽组织充填予以修复,最后演变为瘢痕组织。所以,术后 3 个月时除部分病灶因术后局部血管新生,出现硬度略变软之外,大部分病灶的 E/E₀ 均较术后 1 小时升高。另外我们推测术后某一时间段由于坏死组织液化,会出现肌瘤变软,即 E/E₀ 减小的过程,本研究未对此方向

进行研究。

本研究分别在 2D、RTE、CEUS 条件下对病灶直径进行测量,结果显示术前 RTE 检测病灶直径大于 2D 及 CEUS,术后 1 小时 2D 检测病灶直径大于 RTE 及 CEUS,术后 3 个月 3 种方法检测病灶直径差异无统计学意义。子宫肌瘤膨胀性生长压迫周围的子宫肌层形成假包膜,2D 超声通过肌瘤假包膜及肌瘤组织与周边正常肌组织的声阻抗差识别边界;RTE 检查是根据不同组织的弹性系数差异进行成像,通过图像上病灶与周围正常组织的颜色差异识别边界;CEUS 成像原理是滤除基波成分而有选择性地接受造影剂微泡产生的谐波信号而进行成像,临床通过病灶内部的血流灌注与正常肌组织的差异评估病灶直径,并已得到临床认可。经过分析,本研究中术前部分较软子宫肌瘤弹性成像显示蓝绿相间绿色为主,与周边黄绿色的正常肌组织分界不清晰,导致测量直径较 2D、CEUS 偏大。但是 RFA 治疗后 1 小时,肌瘤假包膜受到破坏,而且治疗所产生的气体尚未完全消散,二维图像受干扰严重,因此显示消融病灶边界常不清晰。国内外也有研究表明消融病灶强回声大小与实际消

融范围无良好的相关性，不能用强回声范围来预测消融范围^[18,19]。RTE 检查不受气体影响，而且由于消融后病灶硬度均较术前增加，所以与周围肌层分界明显，所测直径与 CEUS 下消融病灶无灌注区范围^[20]差异无统计学意义。术后 3 小时，二维图像不再受气体干扰，病灶较之前变硬，故无论在 2D、RTE、CEUS 哪种条件下消融病灶均能较好的显示边界，故三者对病灶直径的评估差异无统计学差异。因此，RTE 检查虽然在术前因受部分较软的肌瘤影响造成对肌瘤大小的评估出现一定偏差，但在用于 RFA 术后消融范围的评估时，可以弥补二维超声的不足，且无创、方便。

在 RFA 治疗中，正确判断消融病灶的消融程度，是保证消融质量及疗效的关键。采用 CEUS 提供的消融病灶的微循环情况评价其消融程度，已得到广大学者公认。本研究中将术后 1 小时及 3 个月时（均为补充消融前）RTE 与 CEUS 结果进行分析，发现以消融病灶蓝绿相间为评判病灶消融不全的标准时，与 CEUS 结果基本一致。但是，研究中发现 RFA 术后 1 小时 5 例病灶、术后 3 个月 4 例病灶两种方法评估结果不一致。弹性图像显示为蓝绿相间，而 CEUS 显示病灶全程无灌注，可能与肌瘤体积及术前硬度相关。肌瘤体积较大时，其受力不均匀，组织产生的形变大小不一，故弹性图像可以表现为蓝绿相间。另外研究表明^[16]质地较软的肌瘤内部细胞成分不均匀，热量容易分散，内部消融不均匀，故血管虽然已全部灭活，但短期内弹性图像仍可能表现为蓝绿相间。弹性图像显示病灶完全被蓝色覆盖，但是 CEUS 呈现不均匀低增强，这种偏差与 RTE 无法评价病灶的血流状态的成像原理有关。周洪雨等^[12]离体动物实验研究表明，弹性图的蓝色区域可代表热消融后组织细胞的凝固性坏死区，但本研究由于肌瘤特殊的组织结构，部分肌瘤术前弹性图像也表现为完全被蓝色覆盖。所以 RFA 治疗后病灶总体硬度较高，但当局部尚有一些微小血管存在活性时，由于 RTE 无法评价消融灶的血流状态，而 CEUS 能清晰的显示小血管内低速、细小血流，因此造成评估结果出现假阴性。本研究认为 RTE 虽尚不能完全取代 CEUS，但可以在 CEUS 之前初步预估病灶消融程度。由于本研究入组病例少，故尚需大量临床及基础研究为 RTE 用于消融病灶消融程度的评估提供定量的诊断指标及依据。

综上所述，RFA 术后肌瘤逐步变硬，RTE 检查能够反映这种硬度变化；RTE 能够评估子宫肌瘤尤其是 RFA 术后病灶的范围并预估消融程度，故 RTE 检查在子宫肌瘤 RFA 治疗中的应用前景可期。

参考文献(References)

- [1] 谢幸, 苟文丽. 妇产科学[M]. 北京: 人民卫生出版社, 2013: 369-372
Xie Xing, Gou Wen-li. Obstetrics and Gynecology [M]. Beijing: People's medical publishing house, 2013: 369-372
- [2] Robles R, Aguirre VA, Argueta AI, et al. Laparoscopic radiofrequency volumetric thermal ablation of uterine myomas with 12 months of follow-up[J]. Int J Gynecol Obstet, 2013, 120(1): 65-69
- [3] Meloni MF, Andreano A, Zimbaro F, et al. Contrast enhanced ultrasound roles in immediate post-procedural and 24-h evaluation of the effectiveness of thermal ablation of liver tumors [J]. J Ultrasound, 2012, 15(4): 207-214
- [4] 谢斌, 王亚琴, 左鹏, 等. 超声造影在高强度聚焦超声治疗子宫肌瘤中的作用评价[J]. 中国超声医学杂志, 2013, 29(8): 754-757
Xie Bin, Wang Ya-qin, Zuo Peng, et al. Contrast-enhanced ultrasound in treatment of ultrasound-guided high intensity focused ultrasound ablation for uterine fibroids [J]. Chinese J Ultrasound Med, 2013, 29(8): 754-757
- [5] 宋彦涛, 董晓秋, 王思明, 等. 基于融合图像的导航技术在子宫肌瘤射频消融术中的初步应用 [J]. 临床超声医学杂志, 2015, 17(12): 793-798
Song Yan-tao, Dong Xiao-qiu, Wang Si-ming, et al. Preliminary application of navigation technology based on fusion image in radiofrequency ablation of uterine fibroids [J]. J Clin Ultrasound Med, 2015, 17(12): 793-798
- [6] 余秀华, 施红, 罗蓉蓉, 等. 二维超声造影评价射频消融治疗子宫肌瘤效果的临床意义[J]. 临床军医杂志, 2011, 39(4): 766-768
Yu Xiu-hua, Shi Hong, Luo Rong-rong, et al. Clinical significance of assessment of the therapeutic effects of hysteromyomas treated with the radiofrequency ablation by two-dimensional contrast-enhanced sonography[J]. Clin J Med Offic, 2011, 39(4): 766-768
- [7] Ophir J, Cespedes I, Ponnekanti H, et al. Elastography: a quantitative method for imaging the elasticity of Biological tissues [J]. Ultrason Imaging, 1991, 13(2): 111-134
- [8] Zhang Y, Tang J, Hang H D, et al. Transrectal real-time tissue elastography--an effective way to distinguish benign and malignant prostate tumors [J]. Asian Pacific journal of cancer prevention, 2014, 15(4): 1831-1835
- [9] 朱林, 周全. 超声弹性成像对甲状腺肿块的诊断进展 [J]. 临床超声医学杂志, 2012, 14(7): 474-475
Zhu Lin, Zhou Quan. Advances of ultrasonic elastography in diagnosis of thyroid mass[J]. J Clin Ultrasound Med, 2012, 14(7): 474-475
- [10] 詹维伟, 宋琳琳. 超声弹性成像技术对甲状腺结节的诊断价值[J]. 现代实用医学, 2013, 25(7): 721-724
Zhan Wei-wei, Song Lin-Lin. The value of ultrasound elastography in the diagnosis of thyroid nodules[J]. Modern Practical Medicine, 2013, 25(7): 721-724
- [11] Ami O, Lamazou F, Mabille M. Real-time transvaginal elastosonography of uterine fibroids [J]. Ultrasound Obstet Gynecol, 2009, 34(2): 486-488
- [12] 叶宝英, 李丽蟾, 陈瑞玉, 等. 子宫肌瘤和局限型腺肌病超声弹性图像特征分析[J]. 临床超声医学杂志, 2014, 16(3): 200-202
Ye Bao-ying, Li Li-chan, Chen Rui-yu. Analysis of the elastosonography of uterine leiomyoma and focal denomyosis[J]. J Clin Ultrasound in Med, 2014, 16(3): 200-202
- [13] 杨竹, 胡丽娜, 王智彪等. 高强度聚焦超声治疗子宫肌瘤的病理学研究[J]. 中华超声影像学杂志, 2003, 12: 674-676
Yang Zhu, Hu Li-na, Wang Zhi-biao, et al. Pathological study in human leiomyomas treated with high-intensity foused ultrasound [J]. Chin J Ultrasonogr, 2003, 12: 674-676
- [14] 周洪雨, 张晶, 徐瑞芳, 等. 微波消融灶组织病理变化与超声弹性成像图对照的实验研究 [J]. 中华医学超声杂志: 电子版, 2013, 10(12): 1031-1035
Zhou Hong-yu, Zhang Jing, Xu Rui-Fang, et al. Comparative research between tissue pathological change and ultrasound elastography image after microwave ablation [J]. Chin J Med Ultrasound (Electronic Edition), 2013, 10(12): 1031-1035

(下转第 4966 页)

- Leukemia, 2017, 31(3): 774-775
- [10] Butler JS, Qiu YH, Zhang N, et al. Low expression of ASH2L protein correlates with a favorable outcome in acute myeloid leukemia [J]. Leuk Lymphoma, 2017, 58(5): 1207-1218
- [11] Parikh BP, Patel SP, Raiya BN, et al. Applicability of a single 5 color cytoplasmic markers tube as primary panel for immunophenotyping of acute leukemia: A Gujarat Cancer and Research Institute experience[J]. Indian J Cancer, 2016, 53(3): 349-352
- [12] Poh SL, Linn YC. Immune checkpoint inhibitors enhance cytotoxicity of cytokine-induced killer cells against human myeloid leukaemic blasts[J]. Cancer Immunol Immunother, 2016, 65(5): 525-536
- [13] Cardarelli F, Bijol V, Chandraker A, et al. Acute myeloid leukemia after kidney transplantation: a case report and literature review [J]. J Bras Nefrol, 2016, 38(4): 455-461
- [14] Challen GA. Dominating the Negative: How DNMT3A Mutations Contribute to AML Pathogenesis[J]. Cell Stem Cell, 2017, 20(1): 7-8
- [15] Kim YJ, Yang JJ, Han Y, et al. A Rare Case of ETV6/MECOM Rearrangement in Therapy-Related Acute Myeloid Leukemia with t(3;12) and Monosomy 7[J]. Clin Lab, 2017, 63(2): 415-418
- [16] Woelich SK, Braun JT, Schoen MW, et al. Efficacy and Toxicity of Induction Therapy with Cladribine, Idarubicin, and Cytarabine (IAC) for Acute Myeloid Leukemia [J]. Anticancer Res, 2017, 37 (2): 713-717
- [17] Lewis TA, Sykes DB, Law JM, et al. Development of ML390: A Human DHODH Inhibitor That Induces Differentiation in Acute Myeloid Leukemia[J]. ACS Med Chem Lett, 2016, 7(12): 1112-1117
- [18] Koh KN, Im HJ, Kim H, et al. Outcome of Reinduction Chemotherapy with a Modified Dose of Idarubicin for Children with Marrow-Relapsed Acute Lymphoblastic Leukemia: Results of the Childhood Acute Lymphoblastic Leukemia (CALL)-0603 Study [J]. J Korean Med Sci, 2017, 32(4): 642-649
- [19] Estey E. Acute Myeloid Leukemia - Many Diseases, Many Treatments [J]. N Engl J Med, 2016, 375(21): 2094-2095
- [20] Khanna G, Damle NA, Agarwal S, et al. Mixed Phenotypic Acute Leukemia (mixed myeloid/B-cell) with Myeloid Sarcoma of the Thyroid Gland: A Rare Entity with Rarer Association - Detected on FDG PET/CT[J]. Indian J Nucl Med, 2017, 32(1): 46-49
- [21] Mehta RS, Chen X, Antony J, et al. Generating Peripheral Blood Derived Lymphocytes Reacting Against Autologous Primary AML Blasts[J]. J Immunother, 2016, 39(2): 71-80
- [22] Raveendran S, Sarojam S, Vijay S, et al. A Case Report of Concurrent IDH1 and NPM1 Mutations in a Novel t (X;2)(q28;p22) Translocation in Acute Myeloid Leukaemia without Maturation (AML-M1) [J]. Malays J Med Sci, 2015, 22(5): 93-97
- [23] Bordon Y. Immunometabolism: Powering down leukaemia [J]. Nat Rev Immunol, 2017, 17(3): 145

(上接第 4970 页)

- [15] 周洪雨, 张晶, 蔡文佳, 等. 实时超声弹性成像评估微波消融组织凝固范围可行性研究[J]. 中国超声医学杂志, 2013, 29(1): 72-74
Zhou Hong-yu, Zhang Jing, Cai Wen-jia, et al. Empirical study on the accuracy of microwave coagulation zone measured by ultrasound elastography[J]. Chinese J Ultrasound Med, 2013, 29(1): 72-74
- [16] 王思明, 董晓秋, 邵小慧, 等. 实时超声弹性成像评估不同回声水平子宫肌瘤射频消融病灶的价值[J]. 中华超声医学杂志, 2017 [Epub ahead of print]
Wang Si-ming, Dong Xiao-qiu, Shao Xiao-hui, et al. Evaluation of radiofrequency ablative lesions by Real-Time Tissue Elastography in different echo intensity of uterine fibroids following radio-frequency ablation[J]. Chin J Med Ultrasound, 2017[Epub ahead of print]
- [17] 卓忠雄. 子宫肌瘤声像图与病理结构定性定量研究 [J]. 临床超声医学杂志, 1992, 8(1): 3-6
Zhuo Zhong-xiong. Qualitative and quantitative study of ultrasonography and pathological structure of uterine leiomyoma [J]. J Clin Ultrasound Med, 1992, 8(1): 3-6
- [18] Leyendecker JR, Dodd GR, Half GA, et al. Sonographically observed echogenic response during intraoperative radiofrequency ablation of cirrhotic livers: pathologic correlation [J]. Am J Roentgenol, 2002, 178: 1147-1151
- [19] 纪莉, 吴凤林. 超声影像评估组织热消融范围的研究进展[J]. 临床超声医学杂志, 2015, 17(4): 258-260
Ji Li, Wu Feng-lin. Review of ultrasound imaging evaluation on the range of thermal ablation [J]. J Clin Ultrasound Med, 2015, 17 (4): 258-260
- [20] 张晶, 关铮, 钱林学, 等. 超声引导经皮微波消融治疗子宫肌瘤临床应用的指南建议 [J]. 中华医学超声杂志: 电子版, 2015, 12 (5): 353-356
Zhang Jing, Guan Zheng, Qian Lin-xue, et al. Guidelines for the clinical application of ultrasound-guided percutaneous microwave ablation for the treatment of uterine fibroids [J]. Chin J Med Ultrasound (ElectroniEdition), 2015, 12 (5): 353-356